

## Hamiltonian dynamics of the two-dimensional lattice $\phi^4$ model

This article has been downloaded from IOPscience. Please scroll down to see the full text article.

1998 J. Phys. A: Math. Gen. 31 3357

(<http://iopscience.iop.org/0305-4470/31/15/004>)

View [the table of contents for this issue](#), or go to the [journal homepage](#) for more

Download details:

IP Address: 171.66.16.121

The article was downloaded on 02/06/2010 at 06:33

Please note that [terms and conditions apply](#).

# Hamiltonian dynamics of the two-dimensional lattice $\varphi^4$ model

Lando Caiani<sup>†||</sup>, Lapo Casetti<sup>¶¶</sup> and Marco Pettini<sup>§+</sup>

<sup>†</sup> Scuola Internazionale Superiore di Studi Avanzati (SISSA/ISAS), via Beirut 2-4, I-10134 Trieste, Italy

<sup>¶</sup> Istituto Nazionale di Fisica della Materia (INFN), Unità di Ricerca del Politecnico di Torino, Dipartimento di Fisica, Politecnico di Torino, Corso Duca degli Abruzzi 24, I-10129 Torino, Italy

<sup>§</sup> Osservatorio Astrofisico di Arcetri, Largo Enrico Fermi 5, I-50125 Firenze, Italy

Received 1 December 1997

**Abstract.** The Hamiltonian dynamics of the classical  $\varphi^4$  model on a two-dimensional square lattice is investigated by means of numerical simulations. The macroscopic observables are computed as time averages. The results clearly reveal the presence of the continuous phase transition at a finite energy density and are consistent both qualitatively and quantitatively with the predictions of equilibrium statistical mechanics. The Hamiltonian microscopic dynamics also exhibits critical slowing down close to the transition. Moreover, the relationship between chaos and the phase transition is considered, and interpreted in the light of a geometrization of dynamics.

## 1. Introduction

The study of the interplay between microscopic, deterministic dynamics and macroscopic statistical behaviour of large Hamiltonian systems is an old subject which dates back to Boltzmann. This subject has mainly been approached by bearing in mind the problem of the dynamical foundations of equilibrium statistical mechanics. In this framework the so-called ergodic problem is the central point: dynamics is studied in the perspective of proving ergodicity and mixing, thus giving a sound foundation to equilibrium statistical mechanics. Despite many efforts in ergodic theory, this goal remains distant, ergodicity and mixing having been proved only for abstract systems such as the Sinai billiard.

However, a different approach is possible: instead of making a statistical assumption and then looking for its justification in the properties of the microscopic dynamics, one can consider dynamics from the very beginning. In practice, instead of considering a particular Hamiltonian system and trying to prove that its dynamics is mixing, one can observe the actual dynamical evolution of the system and measure the time averages of the dynamical observables of interest. In this way the statistical behaviour emerges directly from the dynamics, and one can wonder whether this behaviour is consistent with the predictions of statistical mechanics. In general, such an approach needs a tool that was not available at Boltzmann's times, i.e. a fast computer. In fact, this approach was pioneered by Fermi

<sup>||</sup> During the editing of this paper Lando Caiani tragically died.

<sup>¶¶</sup> E-mail: lapo@polito.it

<sup>+</sup> Also at: INFN, sezione di Firenze, and INFN, unità di Firenze, Largo Enrico Fermi 2, I-50125 Firenze, Italy. E-mail address: pettini@arcetri.astro.it

*et al* [1], who performed, around 1950, the first numerical experiment on the relationship between dynamics and statistical mechanics, using one of the first computing machines, the MANIAC computer at Los Alamos.

The conceptual point of view adopted in this work is that of Fermi *et al*. We consider the dynamics from the very beginning and look at the statistical properties as emerging from the dynamics itself. The main aim of this work is to show that a dynamical approach is worth and can provide some genuinely new understanding of phenomena that are usually treated in the framework of equilibrium statistical mechanics, like phase transitions. We argue that some of the information that is present in the dynamics of a Hamiltonian system, and that is thrown away at the beginning of the statistical-mechanical description, is relevant to the cooperative phenomena that show up in connection with the phase transition. This means that the relevance of dynamics in this context might go well beyond the foundational aspects related with the ergodic problem.

In particular, by studying the dynamics of a paradigmatic system (belonging to the universality class of the two-dimensional Ising model), the  $\varphi^4$  model on a two-dimensional lattice, we are able to show that the dynamical description is not only consistent with the statistical-mechanical results, but also that a Hamiltonian description of dynamical phenomena like the critical slowing down is possible. Moreover, we suggest that a geometrization of Hamiltonian dynamics based on simple tools of Riemannian geometry—originally introduced to describe chaotic dynamics [2–8]—can provide a global description of the dynamical properties that are relevant to the statistical behaviour. We argue that most of these properties are indeed the consequence of the actual geometric structure of the manifolds where the motion takes place. Hence, geometry can not only be a useful tool in the theory of chaos, but hopefully can also provide the correct language to bridge microscopic dynamics and macroscopic statistical behaviour which is still lacking. In particular, phase transitions might be seen as the consequence of some major change in the geometric or even in the topologic structure of the ‘mechanical’ manifolds [9]. Thus, dynamics can introduce new concepts and tools in statistical physics. In our opinion these tools—here applied to a ‘standard’ statistical-mechanical system—might prove useful both on conceptual and practical grounds also dealing with ‘non-standard’ topics in statistical physics, as the emerging field of phase transitions in finite systems (clusters, polymers, proteins) or long-studied but still unsolved problems such as the dynamics and statistical mechanics of glasses and more generally disordered or frustrated systems.

Several other works have recently addressed the problem of the relevance of microscopic Hamiltonian dynamics to phase transitions, in particular in the framework of mean-field-like models [10] and more generally as far as long-range couplings among particles are considered [11]. Moreover, there is now a renewed interest in microcanonical thermodynamics, both on general aspects [12, 13] and on phase transitions [14, 15].

This paper is organized as follows. In section 2 we discuss some general aspects of the problem, then in section 3 the model and the relevant dynamical observables are introduced. Section 4 is devoted to a discussion of the results of the dynamical simulations. In section 6 we briefly recall the main points of the Riemannian theory of Hamiltonian dynamics and then we discuss the peculiar geometric properties of the two-dimensional  $\varphi^4$  lattice model. Finally, in section 7 we draw some conclusions.

## 2. Hamiltonian dynamics and phase transitions

The dynamical aspects of equilibrium phase transitions are usually approached assuming from the outset the formalism of canonical equilibrium statistical mechanics. Dynamics is

introduced only *a posteriori*, and usually use phenomenological, nondeterministic dynamics, e.g. Langevin dynamics [16].

As already stated in the introduction, our approach is different. Given a Hamiltonian system which exhibits a phase transition according to equilibrium statistical mechanics, we wonder what its dynamical behaviour is when it is studied as a natural dynamical system, i.e. associating *a priori* to the system a deterministic (Hamiltonian) dynamics. Accordingly, thermodynamic quantities will be obtained as time averages along the dynamical trajectories, whence—assuming ergodicity at least for the ‘usual’ thermodynamic observables (see [13] for recent results on the dependence of ergodic behaviour on the choice of the observable)—such quantities will be equal to *microcanonical* averages, whereas second-order equilibrium phase transitions are usually studied within the *canonical* ensemble.

The two ensembles are equivalent only in the thermodynamic limit, thus the phenomenology observed in finite systems, as systems considered in numerical simulations necessarily are, might be different. To give only one example, let us consider the phenomenon of *ergodicity breaking*, i.e. the fact that ergodicity might no longer hold in the whole phase space but only in disjoint subsets of it. Such a phenomenon is indeed tightly related to phase transitions; in fact, when it happens, one may observe, as a consequence, a symmetry breaking, as in usual phase transitions. But ergodicity breaking is a more general concept than symmetry breaking, in fact one can recognize ergodicity breaking also as the origin of those phase transitions which do not correspond to the breaking of an evident symmetry of the Hamiltonian (for example in spin glasses) [17]. In the canonical ensemble, ergodicity can be broken only in the thermodynamic limit, while in the microcanonical ensemble, in principle, there might be ergodicity breaking also in finite systems. Ergodicity being a dynamical property, we think that a dynamical approach is particularly appropriate to study such a phenomenon.

In the following we shall present in detail a dynamical study, performed by means of numerical simulations, of the so-called  $\varphi^4$  lattice model with  $\mathbb{Z}_2$  symmetry. The first, preliminary, goal of such a study is to show that the dynamical phenomenology is consistent with the usual statistical description (the model exhibits a continuous phase transition which belongs to the universality class of the Ising model). The main results concern intrinsically dynamical properties, i.e. time correlation functions and Lyapunov exponents, and suggest interesting developments. In particular, two facts emerge: (i) the possibility of a Hamiltonian (i.e. *ab initio*) description of critical dynamics aspects like the critical slowing down, and (ii) a tight relationship between the *local* instability of the dynamics in phase space (characterized by the Lyapunov exponent and the related geometric observables discussed in section 6) on the one side and the *global* phenomenon of the phase transition on the other side. It is worth noticing that a peculiar behaviour of the temperature dependence of the Lyapunov exponent close to a phase transition (actually a Kosterlitz–Thouless transition) was observed for the first time by Butera and Caravati in 1987 [18].

A more detailed discussion of the above-mentioned aspects as well as a discussion of the results can be found in [19].

### 3. Model and dynamical observables

Let us consider a discretized (lattice) version of the classical  $\varphi^4$  field Hamiltonian, which reads as

$$\mathcal{H} = \sum_i \left[ \frac{1}{2} \pi_i^2 + \frac{J}{2} \sum_{j=1}^d (\varphi_{i+j} - \varphi_i)^2 - \frac{1}{2} m^2 \varphi_i^2 + \frac{\lambda}{4!} \varphi_i^4 \right]. \quad (1)$$

According to equilibrium statistical mechanics, the system described by the Hamiltonian (1) has a critical point at finite temperature provided that  $d > 1$ . In the following we will restrict ourselves to the case  $d = 2$ ; the case  $d = 3$  has been considered elsewhere, together with the cases of  $O(n)$ -invariant  $\varphi^4$  models [20].

### 3.1. Dynamics and thermodynamic observables

Our dynamical approach to the model defined by the Hamiltonian (1) is based on the direct solution of the equations of motion—Hamilton's equations—that read as

$$\begin{aligned}\dot{\varphi}_i &= \pi_i \\ \dot{\pi}_i &= J \sum_{\mu=1}^d (\varphi_{i+\mu} + \varphi_{i-\mu} - 2\varphi_i) + m^2 \varphi_i - \frac{1}{3!} \lambda \varphi_i^3.\end{aligned}\quad (2)$$

The numerical integration of the  $2N$  equations (2) has been performed by means of a third-order bilateral symplectic algorithm [21]. The parameters have been chosen as follows:  $J = 1$ ,  $m^2 = 2$ ,  $\lambda = 0.6$ . The average of any observable is defined as a time average, i.e.

$$\langle f \rangle = \lim_{t \rightarrow \infty} \frac{1}{t} \int_0^t f(\varphi(\tau), \pi(\tau)) d\tau.\quad (3)$$

In practice, such an average is evaluated by means of a discrete sampling of  $f$ .

As already discussed in section 2, even if we cannot rigorously prove that the invariant ergodic measure associated with the Hamiltonian dynamics of our system is the microcanonical measure, the microcanonical ensemble is the statistical ensemble which is naturally associated with Hamiltonian dynamics nevertheless, for it is defined directly from the dynamics itself. Thus, in defining the dynamical observables which represent the thermodynamic properties of our model, we shall consider the microcanonical ensemble.

The phase-space density of the microcanonical measure can be written as [22]

$$\rho_{\text{micro}} = \frac{1}{\omega} \delta(\mathcal{H}(\varphi, \pi) - E)\quad (4)$$

where the normalization  $\omega$  is given by

$$\omega = \int \delta(\mathcal{H}(\varphi, \pi) - E) d\varphi d\pi\quad (5)$$

and  $d\varphi d\pi$  is a shorthand for  $d\varphi_1 \dots d\varphi_N d\pi_1 \dots d\pi_N$ .

The entropy  $S$  is defined once the external parameter  $E$  (the energy of the system) is assigned. Different definitions of  $S$  can be given, all of which are equivalent in the thermodynamic limit. The two common definitions are (we set  $k_B = 1$ )

$$S^\Omega(E) = \log \Omega(E)\quad (6)$$

$$S^\omega(E) = \log \omega(E)\quad (7)$$

where

$$\Omega(E) = \int \vartheta(\mathcal{H}(\varphi, \pi) - E) d\varphi d\pi.\quad (8)$$

The temperature is defined thermodynamically as

$$\beta = \frac{1}{T} = \frac{\partial S(E)}{\partial E}\quad (9)$$

in the above definition,  $S$  can denote either  $S^\Omega$  or  $S^\omega$ , whence we have two different definitions of temperature,  $T^\Omega$  and  $T^\omega$ . Again the two definitions are equivalent in the

thermodynamic limit. Let us now limit ourselves to the case of natural dynamical systems, i.e. to Hamiltonian systems with  $N$  degrees of freedom whose Hamiltonian can be written as

$$\mathcal{H} = \sum_{i=1}^N \frac{\pi_i^2}{2m} + V(\varphi) = K + V \tag{10}$$

then the temperature can be expressed in terms of the kinetic energy as follows [23]:

$$T^\Omega = \frac{\Omega}{\omega} = \frac{2}{N} \langle K \rangle \tag{11}$$

$$T^\omega = \left[ \left( \frac{2}{N} - 1 \right) \langle K^{-1} \rangle \right]^{-1}. \tag{12}$$

It is worth noticing that for natural dynamical systems definition (11) also coincides with the definition of temperature in the canonical ensemble. In what follows, unless explicitly stated otherwise, we shall adopt this definition of temperature and we shall drop the superscript  $\Omega$ , i.e.  $T = T^\Omega$ . A more general approach to microcanonical thermodynamics [12] has been recently introduced, which allows us to find new expressions for thermodynamical observables. Anyhow, definition (11) is the best suited for numerical simulations in the case of natural systems [13].

Another thermodynamic quantity to be computed in our simulations is the constant-volume specific heat, defined as

$$\frac{1}{C_v} = \frac{\partial T(E)}{\partial E}. \tag{13}$$

From the definition and equation (11) it follows that [23]

$$c_v = \frac{C_v}{N} = [N - (N - 2) \langle K \rangle \langle K^{-1} \rangle]^{-1} \tag{14}$$

in the thermodynamic limit  $N \rightarrow \infty$  this expression for the specific heat reduces to the well known Lebowitz–Percus–Verlet formula [24],

$$c_v = \frac{1}{2} \left( 1 - \frac{N \langle K^2 \rangle - \langle K \rangle^2}{\langle K \rangle^2} \right)^{-1} \tag{15}$$

which is almost universally used to compute the specific heat in molecular-dynamics simulations [26]. Notice that equation (15) is derived from an asymptotic expansion of the microcanonical fluctuations in terms of the canonical ones, thus it is only valid in the limit of large  $N$ . In contrast, formula (14) is exact at *any* value of  $N$ . Hence, this is the correct expression to be used in a finite system.

Finally, we will consider the order parameter, i.e. the ‘magnetization’

$$\langle \varphi \rangle = \frac{1}{N} \left\langle \sum_{i=1}^N \varphi_i \right\rangle. \tag{16}$$

#### 4. Results of the dynamical simulations

We now turn to the problem of detecting the phase transition in our lattice  $\varphi^4$  Hamiltonian system. According to the thermodynamic definition, we must look for a singularity of the thermodynamic observables as functions of the energy—or better as a function of the energy density  $\varepsilon = E/N$  which remains finite as  $N \rightarrow \infty$  and facilitates the comparison of the results obtained at different lattice sizes. In particular, we look for a singularity in  $c_v(\varepsilon)$ .

Besides, being the transition associated with the spontaneous breaking of the  $\mathbb{Z}_2$  symmetry, we will look for the appearance of a nonzero order parameter, i.e. for a nonvanishing value of the average magnetization  $\langle\varphi\rangle$ .

#### 4.1. Binder cumulants

In the canonical ensemble, a phase transition may occur only in the thermodynamic limit. As long as  $N$  is finite, all the thermodynamic quantities are regular functions of the temperature, and ergodicity and symmetry are not broken. Nevertheless, some marks of the transition clearly show up also in a finite system. The specific heat does not diverge, but exhibits a peak—whose height grows with the size of the system—at a temperature  $T_c^{c_v}(N)$ , while the order parameter is expected to be vanishing in the whole temperature range at any finite value of  $N$ . Nevertheless, this is true only in principle: in practice, for example in a canonical Monte Carlo simulation, where the simulation time is necessarily finite, the system is trapped in one of the two phases for a ‘time’ which grows exponentially with  $N$  [17], and one observes a fictitious symmetry breaking at a temperature  $T_c^\varphi(N)$ . The latter temperature in general does not coincide with  $T_c^{c_v}(N)$ , even if

$$\lim_{N \rightarrow \infty} T_c^{c_v}(N) = \lim_{N \rightarrow \infty} T_c^\varphi(N) = T_c^\infty. \quad (17)$$

In the microcanonical ensemble ergodicity breaking may also occur at finite  $N$ , hence one could expect a ‘true’ critical energy to be defined also at finite  $N$ . No rigorous theoretical result is at disposal as far as this aspect is concerned. Nevertheless, it is reasonable to expect—and this is indeed what is observed—that the actual behaviour of the thermodynamic functions will be similar to the canonical case, at least as  $N$  is sufficiently large. In particular, we expect the specific heat to exhibit a peak at a critical energy density which is a function of  $N$ , and the order parameter to be nonvanishing below another critical energy, again depending on the size of the system.

In the framework of the statistical theory of critical phenomena, finite-size scaling [27] allows us to estimate the critical properties of the infinite system from the values of the thermodynamic observables in finite samples of different sizes. In particular it is possible to locate the critical point by means of the so-called *Binder cumulants* [28]. The Binder cumulant  $g$  is defined for our system as

$$g = 1 - \frac{\langle\varphi^4\rangle}{3\langle\varphi^2\rangle^2}. \quad (18)$$

In the disordered phase the probability distribution of the order parameter will be nearly Gaussian with zero mean, hence  $g \simeq 0$ . At variance, at zero temperature (or energy), when  $\varphi_i \equiv \varphi_0$  with no fluctuations,  $g = \frac{2}{3}$ . At different sizes of the system,  $g(T)$  will decay from  $\frac{2}{3}$  to 0 with different patterns. It is remarkable that the value of  $g$  at  $T_c^\infty$  is *independent* of  $N$ , provided  $N$  is large enough for the scaling regime to set in, hence the critical point is given by the intersection of the different curves  $g(T)$  for different values of  $N$ . In principle, two different sizes are sufficient to locate a transition; in practice, owing to the unavoidable numerical errors which affect  $g$ , it will be necessary to consider three or more values of  $N$ . Moreover, the value of  $g$  at the critical point, usually referred to as  $g^*$ , is a universal quantity; for a simple proof see for example [27].

The theory behind the Binder cumulant method is totally internal to canonical statistical mechanics: to our knowledge, no extension of this theory to the microcanonical ensemble exists. Nevertheless we will adopt the pragmatic point of view of assuming its validity as a numerical tool also in our dynamical simulations, and our operative definition of the critical

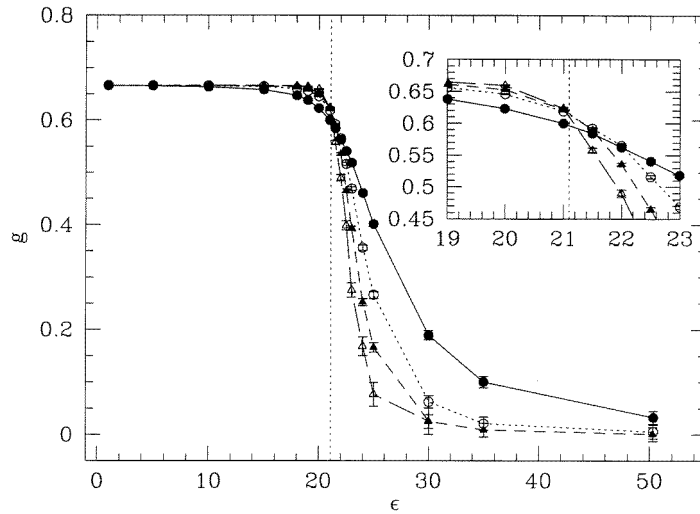


**Figure 1.** Binder cumulants  $g(18)$  versus energy density  $\varepsilon$  for different sizes of the system. The symbols denote respectively  $N = 10^2$  (full circles),  $N = 20^2$  (open circles),  $N = 30^2$  (full triangles),  $N = 50^2$  (open triangles). The vertical dotted line marks the estimated value of  $\varepsilon_c \simeq 21.1$ . The inset shows a magnification of the transition region.

energy density  $\varepsilon_c^\infty$  will be the intersection point of the curves  $g(\varepsilon)$  at different  $N$ . The consistency of the method will be checked *a posteriori*. In the following, unless explicitly stated otherwise,  $\varepsilon_c$  and  $T_c$  will denote respectively  $\varepsilon_c^\infty$  and  $T_c^\infty$ .

The results for  $g(\varepsilon)$  at different sizes for the two-dimensional lattice  $\varphi^4$  model are shown in figure 1. The crossing of the various curves at  $\varepsilon_c \simeq 21.1$  is evident.

## 4.2. Thermodynamical observables

**4.2.1. Temperature.** The temperature of the two-dimensional  $\varphi^4$  system, numerically determined according to equation (11), is plotted in figure 2. Notice the change in the convexity of the function  $T(\varepsilon)$  at  $\varepsilon = \varepsilon_c$ .

In figure 3 a comparison between the temperatures computed according to the two definitions (11) and (12) is shown. It is evident that already in a  $10 \times 10$  lattice the two temperatures are practically identical.

In figure 4 the Binder cumulants are plotted versus temperature  $T$  to locate the critical temperature  $T_c$ . We see that this  $T_c$  is consistent with  $T(\varepsilon_c)$ .

**4.2.2. Specific heat.** The specific heat of the two-dimensional  $\varphi^4$  system is plotted versus energy density in figure 5. The asymptotic values of the specific heat in the limits  $\varepsilon \rightarrow 0$  and  $\varepsilon \rightarrow \infty$  are exactly known. In fact at low energies the anharmonic terms in the Hamiltonian can be neglected, the system behaves as a collection of harmonic oscillators and  $c_v \approx 1$ . In the high-energy limit the quadratic terms in the potential are negligible with respect to the quartic ones, whence  $c_v \approx \frac{1}{2} + \frac{1}{4} = \frac{3}{4}$ . At intermediate energy densities, a neat peak shows up whose position is close to  $\varepsilon_c$ . The height of the peak grows with  $N$ .

**4.2.3. Order parameter.** Let us turn to the behaviour of the order parameter  $\langle \varphi \rangle$ . In principle, a nonzero value of  $\langle \varphi \rangle$  is the characteristic signal of the breaking of the  $\mathbb{Z}_2$



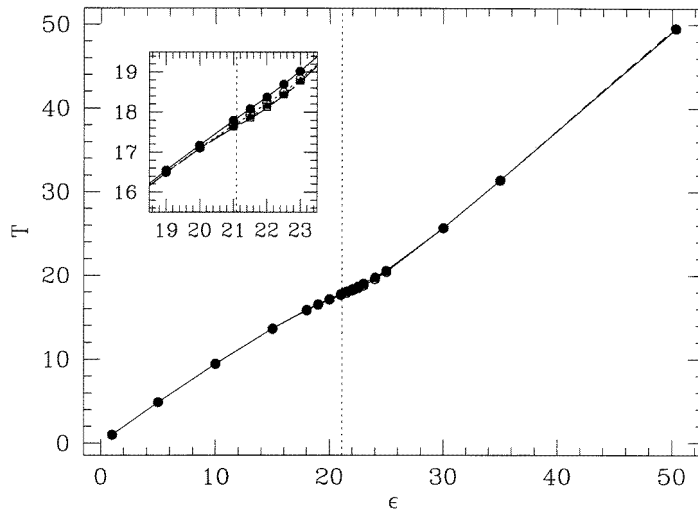


**Figure 2.** Temperature  $T$  versus energy density  $\varepsilon$ . Symbols as in figure 1.

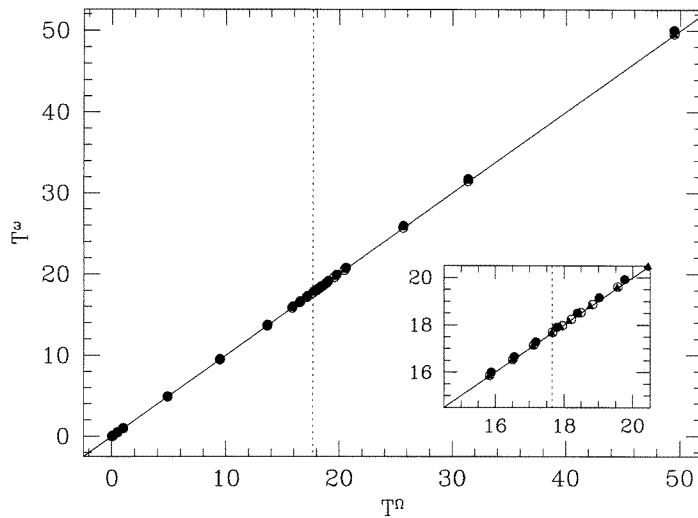


**Figure 3.** Comparison of the two different definitions of temperature  $T = T^\Omega$ —equation (11), full circles—and  $T = T^\omega$ —equation (12), squares—at three different lattice sizes:  $N = 10^2$  (full circles),  $N = 20^2$  (open circles),  $N = 30^2$  (full triangles). The full line is the line  $T^\omega = T^\Omega$ , the dotted vertical line marks the estimated value of  $T_c$  (see figure 4).

symmetry, which is in turn a consequence of ergodicity breaking. In practice, as long as a finite system is considered, the situation is more subtle. We have already observed that in a canonical ensemble, where the temperature is fixed, ergodicity can only be broken in the thermodynamic limit, hence the eventual appearance of a nonzero order parameter is a consequence of the necessarily finite observation time. In order to obtain reliable results the standard procedure is then to compute  $\langle |\varphi| \rangle$  rather than  $\langle \varphi \rangle$ ; in this way one has a quantity whose average is always nonnegative, and that coincides with the ‘true’ order parameter as  $N \rightarrow \infty$ . Obviously in the symmetric phase this quantity, at finite  $N$ , is nonzero: its

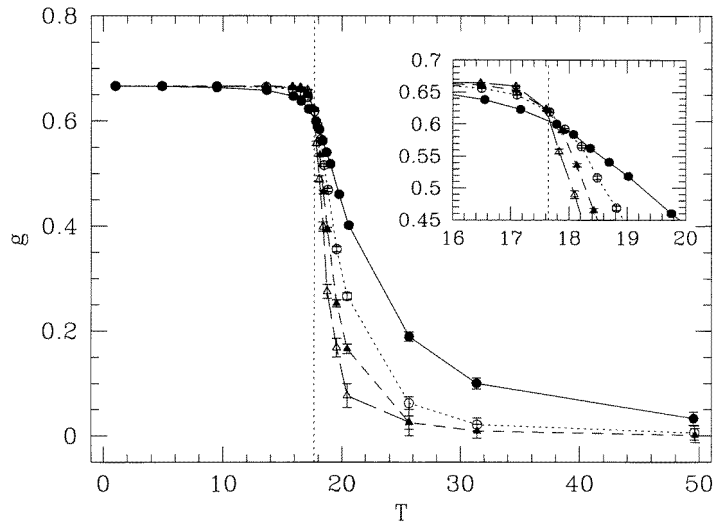


**Figure 4.** Binder cumulants  $g$  (18) versus temperature  $T$ . Symbols as in figure 1. The vertical dotted line marks the estimated value of  $T_c \simeq 17.65$ . The inset shows a magnification of the transition region.

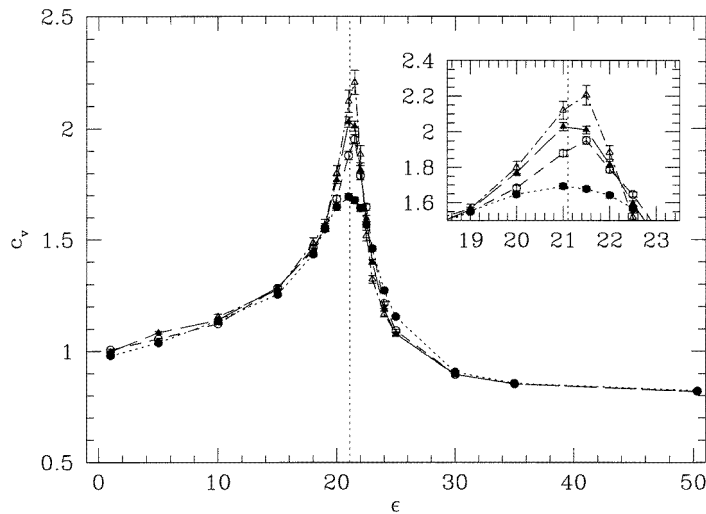


**Figure 5.** Specific heat  $c_p$  versus energy density  $\varepsilon$ . Symbols as in figure 1.

amplitude will decrease as  $1/\sqrt{N}$ . This is precisely the behaviour of our numerical results reported in figure 6.

In the microcanonical ensemble the situation is more complicated, in fact ergodicity breaking is no longer forbidden at finite  $N$ , hence a nonzero value of  $\langle \varphi \rangle$  might be either a finite-time artefact or a ‘true’ signal of symmetry breaking. Anyhow, the mere observation of the result is not sufficient to discriminate between these two alternatives. The order parameter (the ‘true’ one, whose absolute value is taken only *after* the average for graphical reasons) is reported in figure 7. We see that at each  $N$  there is a value of  $\varepsilon$  below which the symmetry appears to be broken, and the value of  $\langle \varphi \rangle$  seems to move almost abruptly

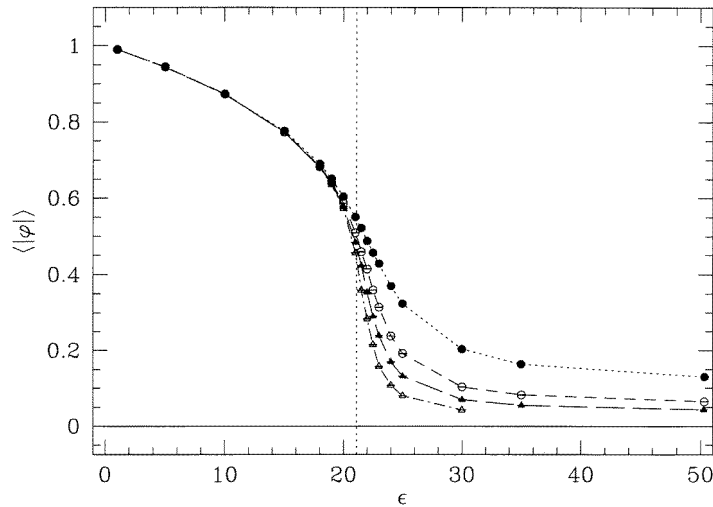


**Figure 6.** Absolute magnetization  $\langle |\varphi| \rangle$  versus energy density  $\varepsilon$ . Symbols as in figure 1.

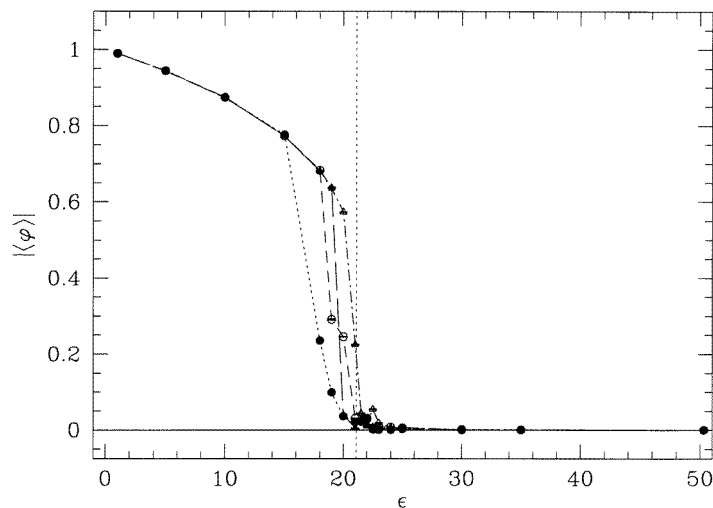


**Figure 7.** Magnetization  $\langle \varphi \rangle$  versus energy density  $\varepsilon$ . Symbols as in figure 1.

from zero to a finite value. These ‘critical’ energy densities are the closer to  $\varepsilon_c$  the larger  $N$  is.

#### 4.3. Critical behaviour

The classical lattice  $\varphi^4$  model, whose Hamiltonian is invariant under a discrete  $\mathbb{Z}_2$  symmetry, belongs to the universality class of the Ising model.

Our goal is not to obtain a precise measurement of the critical exponents, but only to check the consistency of our dynamical results with the statistical theory. The fact that the  $\varphi^4$  theory belongs to the Ising universality class is a great advantage, because the critical exponents of the Ising model in two dimensions have been computed exactly: in particular,

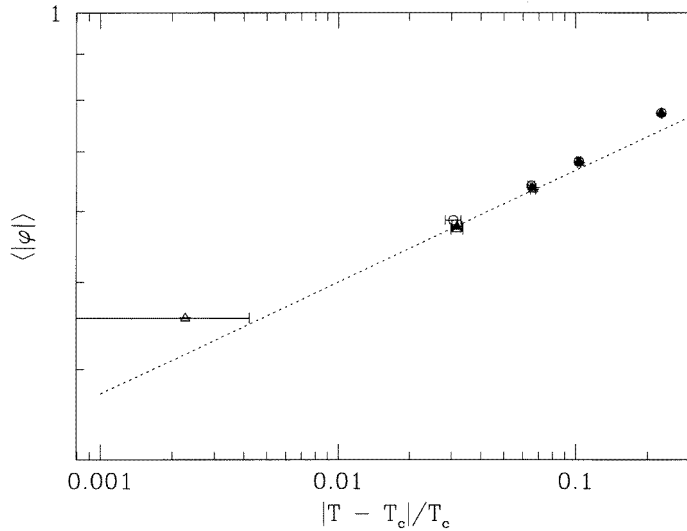


**Figure 8.** Scaling behaviour of the order parameter in the two-dimensional  $\varphi^4$  model. Symbols as in figure 1; only  $20^2$ ,  $30^2$  and  $50^2$  lattices are considered. The dotted line is the exact result for the Ising model, i.e. the power law  $|T - T_c|^{1/8}$ .

the order parameter critical exponent is  $\beta = \frac{1}{8}$  and the specific heat one is  $\alpha = 0$  (the specific heat has a logarithmic singularity). We can compare the numerical outcomes of our simulations with the predicted Ising values in order to check whether the dynamically simulated critical behaviour is compatible with the predictions of statistical mechanics. In figures 8 and 9 the scaling behaviours of the order parameter and of the specific heat are compared with the exact Ising behaviours in two dimensions. The results are clearly very well compatible with the theory. This is a sign that the dynamical approach effectively reproduces the thermodynamical phase transition of the  $\varphi^4$  model.

## 5. Dynamical properties

Heretofore we have shown that the outcomes of the dynamical numerical simulations are perfectly consistent, both qualitatively and quantitatively, with the theoretical expectations regarding the phase transition of the  $\varphi^4$  model. Although obtained through dynamics, all these results deal with equilibrium time averages: the time variable, even if not eliminated from the very beginning as in the statistical approach, has been integrated out in the averaging procedure. Now, we can also wonder whether there are intrinsically dynamical properties of our system that are relevant for the phase transition itself. Moreover, since from our point of view ergodicity breaking has its origin in the dynamics, we can try to understand what features are associated to a Hamiltonian ergodicity breaking.

### 5.1. Time correlation functions

The first dynamical property that we are going to study is the dynamics of the order parameter  $\varphi(t)$ . A qualitative understanding of what is going on is already provided by the time series  $\varphi(t)$  itself: some examples are reported in figure 10 for various values of  $\varepsilon$ , in the case of a  $20 \times 20$  lattice. However, much more interesting information is contained

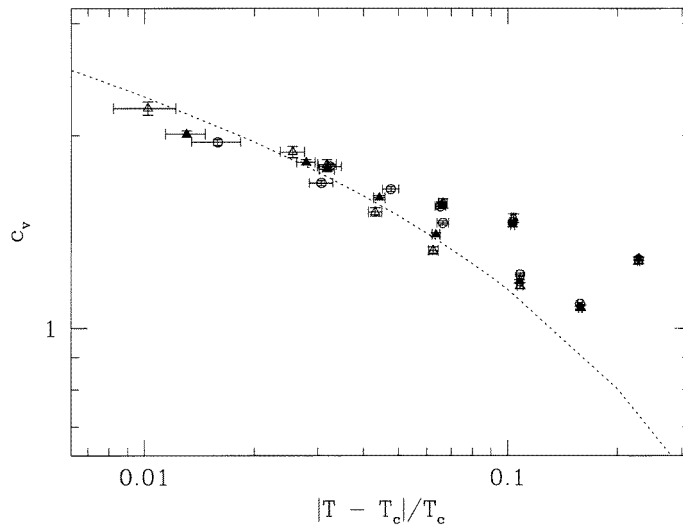


**Figure 9.** The same as in figure 8 for the specific heat. Here the dotted line is the logarithmic behaviour.

in the time correlation functions of the order parameter,

$$C_\varphi(\tau) = \frac{\langle \varphi(t)\varphi(t + \tau) \rangle}{\langle \varphi^2(t) \rangle} \quad (19)$$

some of these functions are plotted in figure 11. We immediately note that close to the critical energy—and indeed very close to the ‘finite  $N$ ’ critical energy where ergodicity appears to be broken according to figure 7—the shape of the correlation function changes rather sharply from an oscillatory pattern with a superimposed decay to a pattern indicating that the values of  $\varphi(t)$  are correlated over an extremely long period of time. Such a phenomenon is obviously reminiscent of *critical slowing down*. The latter is a feature of the local<sup>†</sup> phenomenological dynamical evolutions, for example Monte Carlo dynamics, constructed in order to have the Boltzmann distribution  $e^{-\beta\mathcal{H}}$  as limiting invariant probability distribution, when the system described by  $\mathcal{H}$  is close to a continuous phase transition. The usual explanation for the critical slowing down is that it is a consequence of the divergence of the static correlation length at the phase transition. However, we are now considering a deterministic Hamiltonian microscopic dynamics and not a phenomenological Monte Carlo dynamics, hence our results clearly show that some kind of critical slowing down also exists in the microscopic natural dynamics. Something similar, i.e. the development of low-frequency collective oscillations, was observed in a planar mean-field Heisenberg model close to criticality [10]. This result suggests that a Hamiltonian description of critical slowing down is possible and it might be very useful in dynamically understanding the phenomenon of ergodicity breaking (the study of a simple model which provides a first step towards this Hamiltonian approach to critical slowing down is presented in [19]).

In order to obtain synthetic information from the time correlation functions, let us define a characteristic time  $\tau$  as follows:

$$\tau = \int_0^{t_0} C_\varphi(t) dt \quad (20)$$

<sup>†</sup> There are indeed ‘smart’ dynamics which greatly reduce, or completely eliminate, the critical slowing down; the common feature of these dynamical rules is that of being highly nonlocal [30].

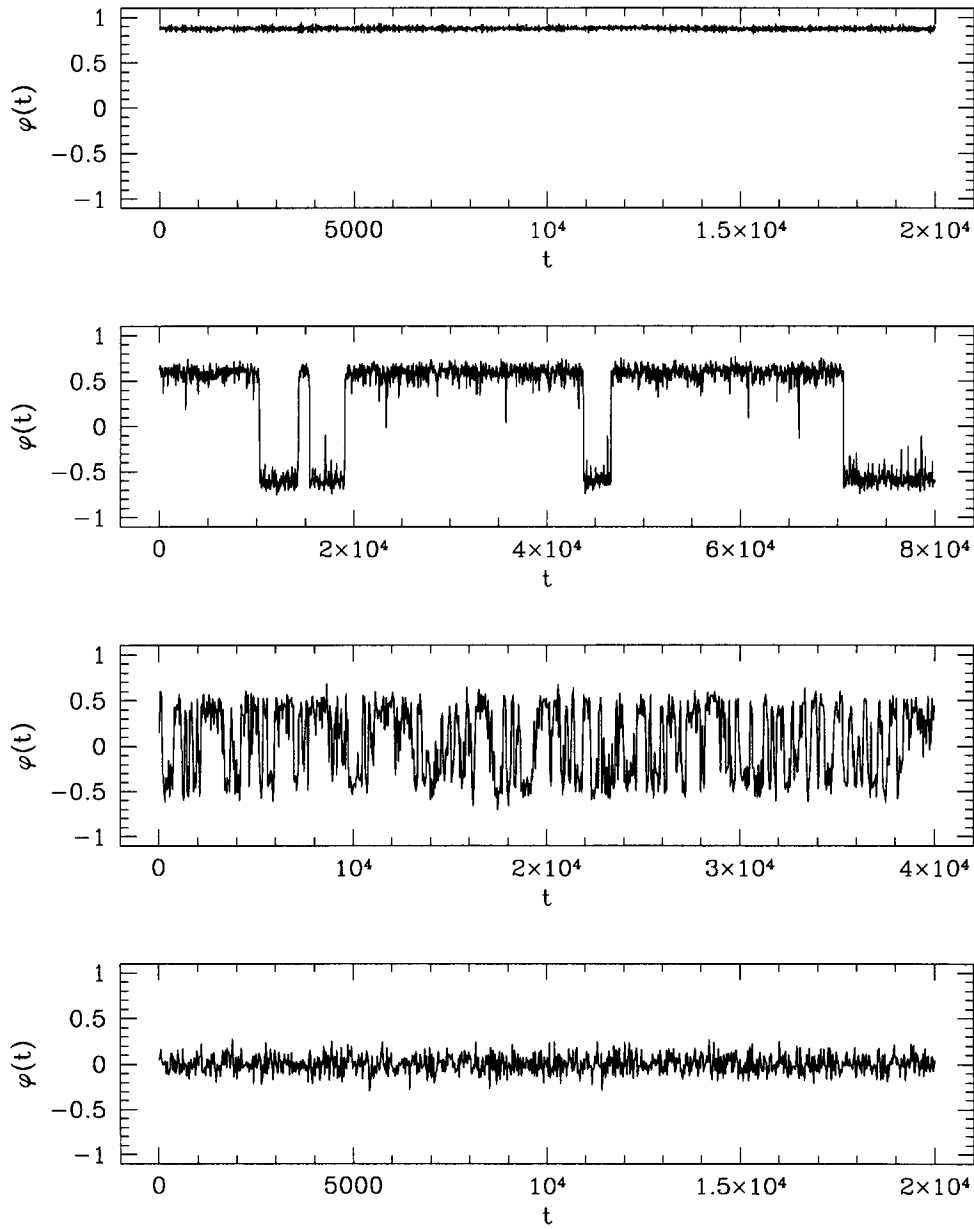


**Figure 10.** Temporal behaviour of the order parameter  $\varphi(t)$  for a  $20^2$  lattice at different values of  $\varepsilon$ : from top to bottom,  $\varepsilon = 10, 20, 22.5$  and  $35$ .

where  $t_0$  is the time where  $C_\varphi$  has its first zero. Such a definition is to a large extent arbitrary, nevertheless it provides a relevant timescale whether the correlation function is oscillatory with typical frequency  $\omega$  and with only a weak damping—as it happens at low energy—in which case  $\tau \approx \omega^{-1}$ , or in the case of an exponentially decaying correlation with inverse time constant  $\gamma$ , in which case  $\tau \approx \gamma^{-1}$ . The values of  $\tau$  computed with Hamiltonian dynamics are reported in figure 12. The striking result is that the characteristic

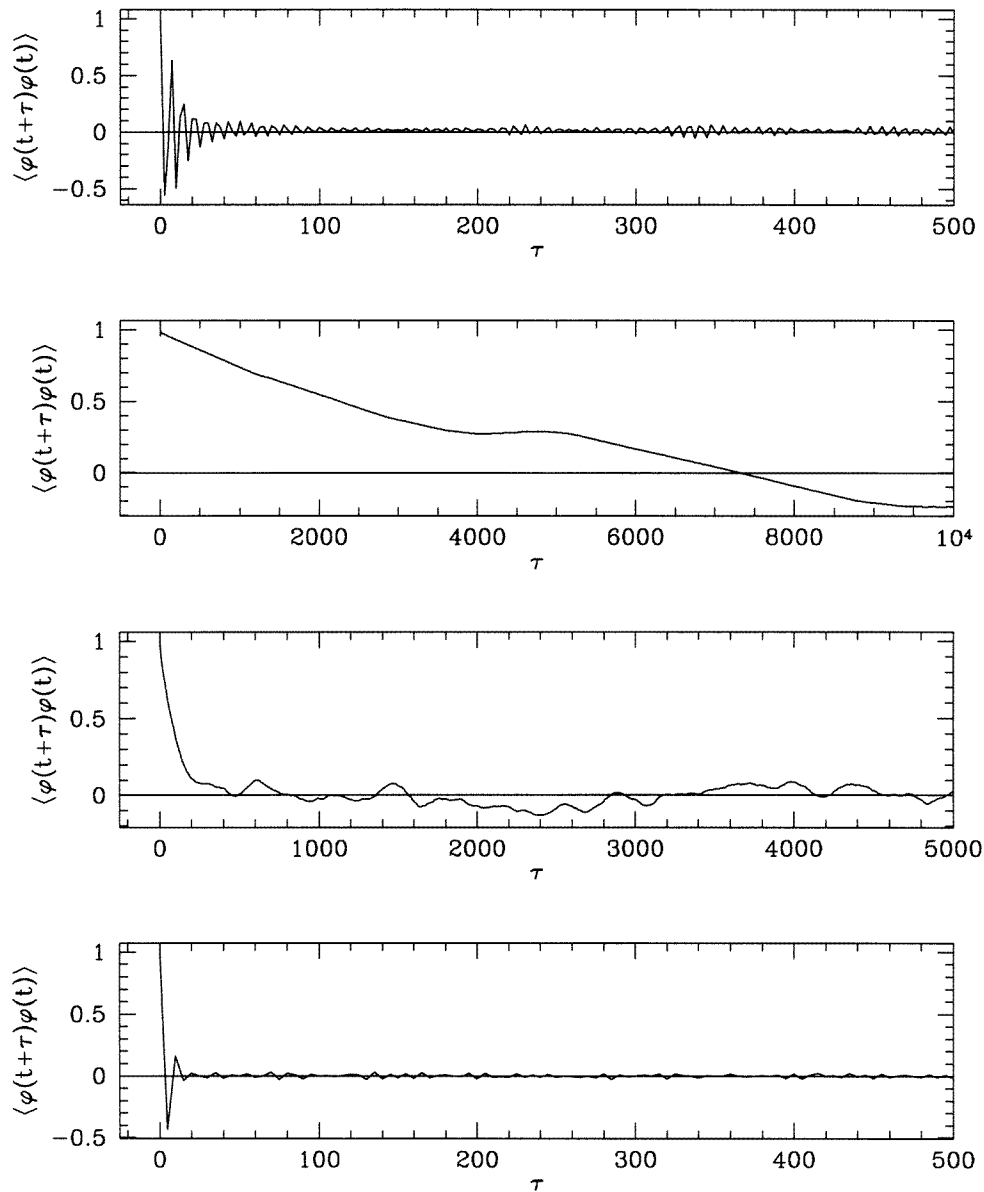


**Figure 11.** Time autocorrelation function of the order parameter  $\varphi(t)$  for the same lattice and at the same energies as in figure 10.

time is rapidly growing (notice the logarithmic vertical axis) as the system approaches the phase transition: the position of the peak is close to the ‘finite  $N$ ’ critical energy.

### 5.2. Chaotic dynamics

The lattice  $\varphi^4$  model is a nonintegrable dynamical system. In the two limits  $\varepsilon \rightarrow 0$  and  $\varepsilon \rightarrow \infty$ , the system is integrable. The two integrable limits respectively represent

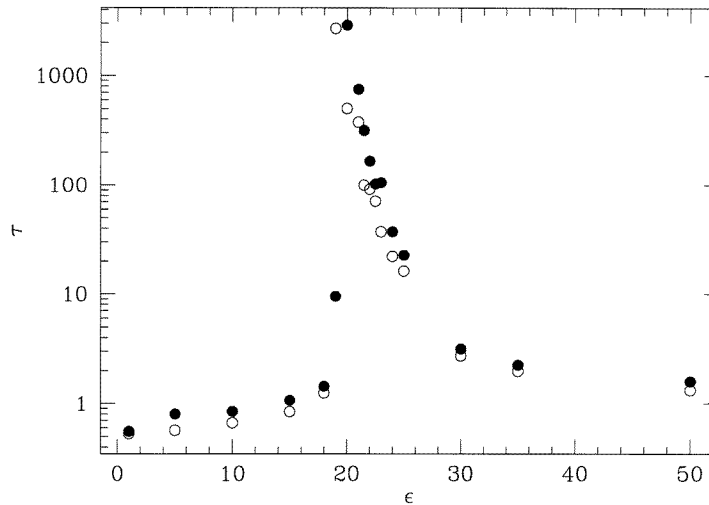


**Figure 12.** Characteristic time  $\tau$  of the order parameter  $\varphi(t)$  (see text). Open circles:  $10^2$  lattice, full circles:  $20^2$  lattice.

a system of coupled harmonic oscillators and a system of independent quartic oscillators. The dynamics will always be chaotic in the whole energy range. Nevertheless, in analogy with other nonlinear oscillator systems, we expect that as the energy density is varied there exist different dynamical regimes characterized by different behaviours of the Lyapunov exponent  $\lambda$ . In particular, the following questions naturally arise. Is there any peculiar behaviour of the Lyapunov exponent in correspondence with the phase transition? Is there any transition between different chaotic regimes in the  $\varphi^4$  lattice model, and, if yes, is there any relationship between these different dynamical regimes and the thermodynamic phases?

There are not yet general and conclusive answers to these questions. Even if the study of a possible relation between chaos and phase transitions is a rather recent issue, which started with the already mentioned pioneering work by Butera and Caravati [18], very different results have already appeared in the literature, ranging from the claim of the discovery of a ‘universal’ divergence in  $\lambda$  as the system approaches criticality in a class of models describing clusters of particles [31], to the observation that the Lyapunov exponent attains its minimum in correspondence with the phase transition in Ising-like coupled map lattices [32], to the apparent insensitivity to the liquid–solid phase transition of the Lyapunov spectra of hard-sphere and Lennard-Jones systems [15]; for other recent results on first-order transitions see [33].

More recently, some very interesting results have been obtained concerning mean-field-like models, in particular globally coupled rotators. Numerical results [34], though of not easy interpretation due to strong finite-size effects, indicate that in these systems, that undergo a mean-field phase transition at a critical energy density  $\epsilon_c$ , the Lyapunov exponent vanishes in the whole disordered phase, whereas it is positive in the low-energy (ordered) phase. Such a result has been theoretically confirmed in a very recent work [35]. Since the latter work is based on the application of the theoretical tools described in section 6, we will discuss there its results.

Our simulation results are plotted in figure 13. The first numerical evidence is that there is a strong dependence of  $\lambda$  on  $N$ , which is peculiar of the presence of a phase transition. Moreover, at large  $N$  a maximum of  $\lambda(\epsilon)$  develops which eventually seems to move towards



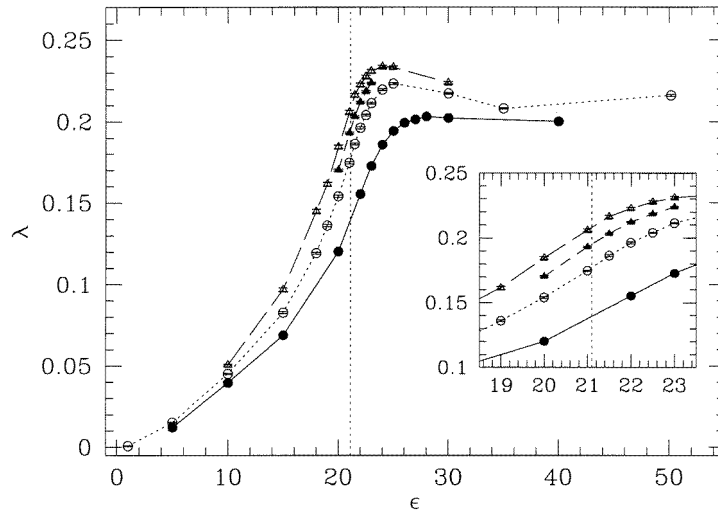


**Figure 13.** Lyapunov exponent  $\lambda$  versus energy density  $\varepsilon$ . Symbols as in figure 1.

the critical energy density. Nevertheless no sharp, or singular, transition between different behaviours is found near  $\varepsilon_c$ , at variance with the three-dimensional case [20]; it is possible that such a sharp transition shows up as  $N \rightarrow \infty$ , but no clear indications of this fact are provided by our results. Nevertheless the behaviour of  $\lambda(\varepsilon)$  in the region  $\varepsilon < \varepsilon_c$  is very different from that of the thermodynamically disordered region, i.e. in the former  $\lambda$  rapidly grows with  $\varepsilon$ , while in the latter it has a quasiflat shape (which is expected to become a decrease as  $\varepsilon$  is large enough, because the high-energy limit is an integrable limit for the model). This behaviour is more clearly shown in figure 14 where a wider energy range is considered and logarithmic axes are used. This suggests that the phase transition has a dynamical counterpart in a passage between different chaotic regimes. However—at present—this statement cannot be formulated in a conclusive way, mainly because there is no clear and unique way to define and characterize a transition between different chaotic regimes (a recent improvement towards an unambiguous characterization of this kind of transitions can be found in [13]).

Moreover, numerical experiments show that the detailed behaviour of the Lyapunov exponent close to the transition does not show ‘universal’ features, i.e. it depends on the details of the Hamiltonian: in contrast, in the low-energy range also for the  $\varphi^4$  model we have  $\lambda \propto \varepsilon^2$  that is the same behaviour observed in most, if not all, of the systems of coupled oscillators. Hence, it is still unclear which feature of the  $\varepsilon$ -dependence of the Lyapunov exponent has to be related with the phase transition. An exception is the already-mentioned case of the mean-field rotators model [34], where the order-disorder phase transition finds its counterpart in a chaos-order dynamical transition: this rather counterintuitive fact can be explained theoretically [35] and is likely to be a peculiarity of mean-field models. We shall return to this issue in the following, in particular in section 6 where we will consider geometric properties which are strictly related with chaotic dynamics, and which, indeed, exhibit a much clearer behaviour near  $\varepsilon_c$ .

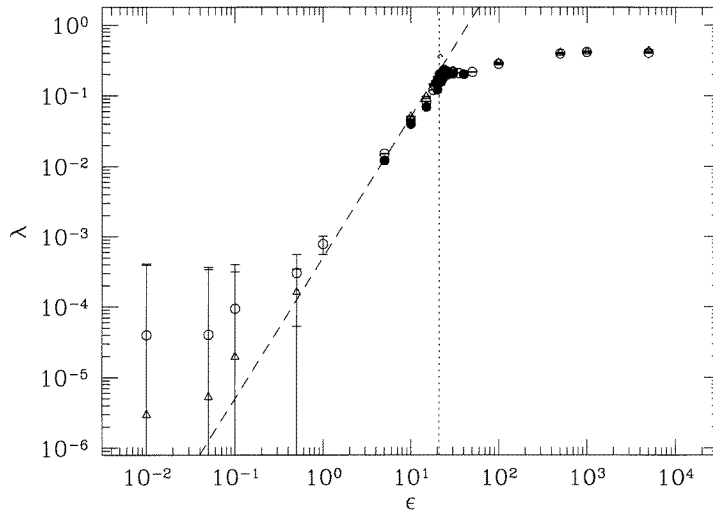


**Figure 14.** The same as in figure 13 in a wider energy range and using logarithmic scales. The broken line is the power law  $\lambda \propto \varepsilon^2$ .

### 6. Geometry of dynamics in the $\varphi^4$ model

Let us turn to the geometrization of the dynamics and its relations with the dynamical description of the phase transition. We will not go into detail, we recall only the notations and main results: all the details can be found in [8] and references therein.

The geometrical formulation of the dynamics of conservative systems was first used by Krylov in his studies on the dynamical foundations of statistical mechanics [36] and subsequently became a standard tool to study abstract systems in ergodic theory. Several new contributions to this subject have recently appeared [2, 3, 7, 8].

Let us briefly recall that the geometrization of the dynamics of  $N$ -degrees-of-freedom systems defined by a Lagrangian  $\mathcal{L} = T - V$ , in which the kinetic energy is quadratic in the velocities:

$$T = \frac{1}{2} a_{ij} \dot{q}^i \dot{q}^j \tag{21}$$

stems from the fact that the natural motions are the extrema of the Hamiltonian action functional  $\mathcal{S}_H = \int \mathcal{L} dt$ , or of the Maupertuis' action  $\mathcal{S}_M = 2 \int T dt$ . In fact also the geodesics of Riemannian and pseudo-Riemannian manifolds are the extrema of a functional: the arc-length  $\ell = \int ds$ , with  $ds^2 = g_{ij} dq^i dq^j$ , hence a suitable choice of the metric tensor allows the identification of the arc-length with either  $\mathcal{S}_H$  or  $\mathcal{S}_M$ , and of the geodesics with the natural motions of the dynamical system. Starting from  $\mathcal{S}_M$  the 'mechanical manifold' is the accessible configuration space endowed with the Jacobi metric

$$(g_J)_{ij} = [E - V(\{q\})] a_{ij} \tag{22}$$

where  $V(q)$  is the potential energy and  $E$  is the total energy. A description of the extrema of Hamilton's action  $\mathcal{S}_H$  as geodesics of a 'mechanical manifold' can be obtained using Eisenhart's metric [37] on an enlarged configuration spacetime ( $\{q^0 \equiv t, q^1, \dots, q^N\}$  plus one real coordinate  $q^{N+1}$ ), whose arc-length is

$$ds^2 = -2V(\{q\})(dq^0)^2 + a_{ij} dq^i dq^j + 2dq^0 dq^{N+1}. \tag{23}$$

The manifold has a Lorentzian structure and the dynamical trajectories are those geodesics satisfying the condition  $ds^2 = C dt^2$ , where  $C$  is a positive constant. In the geometrical framework, the (in)stability of the trajectories is the (in)stability of the geodesics, and it is completely determined by the curvature properties of the underlying manifold according to the Jacobi equation [38]

$$\frac{D^2 J^i}{ds^2} + R^i{}_{jkm} \frac{dq^j}{ds} J^k \frac{dq^m}{ds} = 0 \quad (24)$$

whose solution  $J$ , usually called Jacobi or geodesic variation field, locally measures the distance between nearby geodesics;  $D/ds$  stands for the covariant derivative along a geodesic and  $R^i{}_{jkm}$  are the components of the Riemann curvature tensor. Using the Eisenhart metric (23) the relevant part of the Jacobi equation (24) is [3, 8]

$$\frac{d^2 J^i}{dt^2} + R^i{}_{0k0} J^k = 0 \quad i = 1, \dots, N \quad (25)$$

where the only nonvanishing components of the curvature tensor are  $R_{0i0j} = \partial^2 V / \partial q_i \partial q_j$ . Equation (25) is the tangent dynamics equation which is commonly used to measure Lyapunov exponents in standard Hamiltonian systems. Having recognized its geometric origin, in [8], it has been devised as a geometric reasoning to derive from equation (25) an *effective* scalar stability equation that *independently* of the knowledge of dynamical trajectories provides an average measure of their degree of instability. This is based on two main assumptions: (i) that the ambient manifold is *almost isotropic*, i.e. the components of the curvature tensor—that for an isotropic manifold (i.e. of constant curvature) are  $R_{ijkl} = k_0(g_{ik}g_{jm} - g_{im}g_{jk})$ ,  $k_0 = \text{constant}$ —can be approximated by

$$R_{ijkl} \approx k(t)(g_{ik}g_{jm} - g_{im}g_{jk}) \quad (26)$$

along a generic geodesic  $\gamma(t)$ ; (ii) that in the large  $N$  limit the ‘effective curvature’  $k(t)$  can be modelled by a Gaussian and  $\delta$ -correlated stochastic process. The mean  $k_0$  and variance  $\sigma_k$  of  $k(t)$  are given by the average and the r.m.s. fluctuation of the Ricci curvature  $k_R = K_R/N$  along a geodesic:

$$k_0 = \langle K_R \rangle / N \quad (27a)$$

$$\sigma_k^2 = \langle (K_R - \langle K_R \rangle)^2 \rangle / N. \quad (27b)$$

The Ricci curvature along a geodesic is defined as

$$K_R = \frac{1}{v^2} R_{ij} \frac{dq^i}{dt} \frac{dq^j}{dt} \quad (28)$$

where  $v^2 = \frac{dq^i}{dt} \frac{dq_i}{dt}$  and  $R_{ij} = R^k{}_{ikj}$  is the Ricci tensor; in the case of Eisenhart metric it is

$$K_R \equiv \Delta V = \sum_{i=1}^N \frac{\partial^2 V}{\partial q_i^2}. \quad (29)$$

The final result is the replacement of equation (25) with the aforementioned effective stability equation which is independent of the dynamics and is in the form of a stochastic oscillator equation [7, 8]

$$\frac{d^2 \psi}{dt^2} + k(t) \psi = 0 \quad (30)$$

where  $\psi^2 \propto |J|^2$ . The exponential growth rate  $\lambda$  of the solutions of equation (30), which is therefore an estimate of the largest Lyapunov exponent, can be computed exactly:

$$\lambda = \frac{\Lambda}{2} - \frac{2k_0}{3\Lambda} \quad \Lambda = \left( 2\sigma_k^2\tau + \sqrt{\frac{64k_0^3}{27} + 4\sigma_k^4\tau^2} \right)^{\frac{1}{3}} \quad (31)$$

where  $\tau = \pi\sqrt{k_0}/(2\sqrt{k_0(k_0 + \sigma_k)} + \pi\sigma_k)$ ; in the limit  $\sigma_k/k_0 \ll 1$  one finds

$$\lambda \propto \sigma_k^2. \quad (32)$$

The latter result is the deep origin of the vanishing of the Lyapunov exponent in the whole disordered phase of a mean-field rotator model [34]; in fact, in that model, the curvature fluctuations can be analytically computed and turn out to be nonzero in the low-energy region but vanishing in the whole high-energy phase [35], consistently with the mean-field character of the model. At the critical energy  $\sigma_k$  is discontinuous. The work reported in [35] is particularly important because it is the first example in which the relationship between chaos and phase transitions is theoretically investigated within a framework which allows analytical calculations. The power of the geometric approach is evident in that case.

It is natural to wonder whether the curvature fluctuations show any remarkable (singular) behaviour also in correspondence with nonmean-field phase transitions. Numerical results suggesting a positive answer to this question have already been found in the cases of planar spin models [9] and three-dimensional  $O(n)$   $\varphi^4$  models [20]; in correspondence with a second-order phase transition the curvature fluctuations show a cusp-like behaviour in all the cases considered up until now. These singular behaviours of the curvature fluctuations have been conjectured to be a consequence of a major change in the global geometry, if not in the topology, of the mechanical manifolds.

In the following we are going to show that also in the case of the two-dimensional  $\varphi^4$  lattice theory the above scenario is confirmed. Moreover, we will present some results concerning other geometric quantities, different from those defined in the framework of Eisenhart's metric; these results lend strong support to the topologic interpretation of the apparently singular behaviour of the curvature fluctuations.

### 6.1. Curvature fluctuations with Eisenhart's metric

In the case of the lattice  $\varphi^4$  theory (1) the Ricci curvature per degree of freedom of the Eisenhart metric is

$$k_R = \frac{K_R}{N} = 2dJ - m^2 + \frac{1}{N} \sum_{i=1}^N \frac{\lambda}{2} \varphi_i^2. \quad (33)$$

The time average  $k = \langle k_R \rangle$  of  $k_R$  is plotted versus the energy density for the two-dimensional model in figure 15. It is evident that  $k(\varepsilon)$  changes its convexity close to  $\varepsilon_c$ , hence it shares this feature with the temperature. Anyhow in other models the shape of  $k(\varepsilon)$  is completely different.

What is more interesting, and, in the light of the above discussion, much more significant, is the behaviour of the fluctuations  $\sigma_k^2$ , reported in figure 16. Actually in this figure the normalized fluctuation  $\sigma_k/k$  is reported. A cusp-like behaviour of the curvature fluctuations is evident in correspondence of the critical energy.

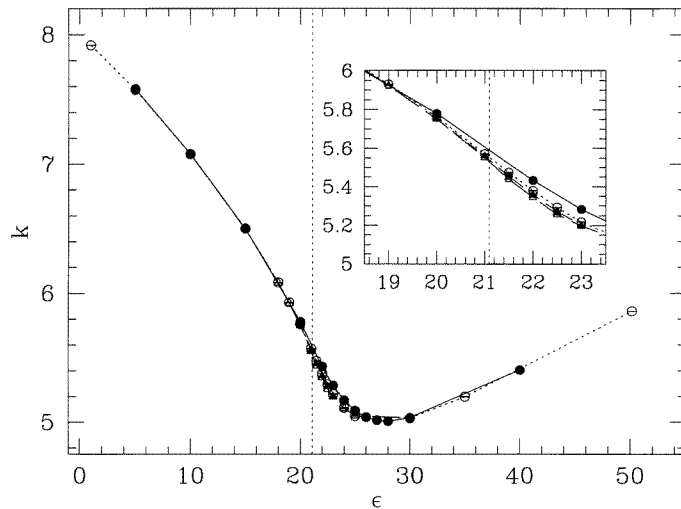


**Figure 15.** Average Ricci curvature  $k$  (33) with Eisenhart metric versus energy density  $\epsilon$  for different sizes of the system. The symbols denote respectively  $N = 10^2$  (full circles),  $N = 20^2$  (open circles),  $N = 30^2$  (full triangles),  $N = 50^2$  (open triangles). The vertical dotted line marks the estimated value of  $\epsilon_c$ . The inset shows a magnification of the transition region.

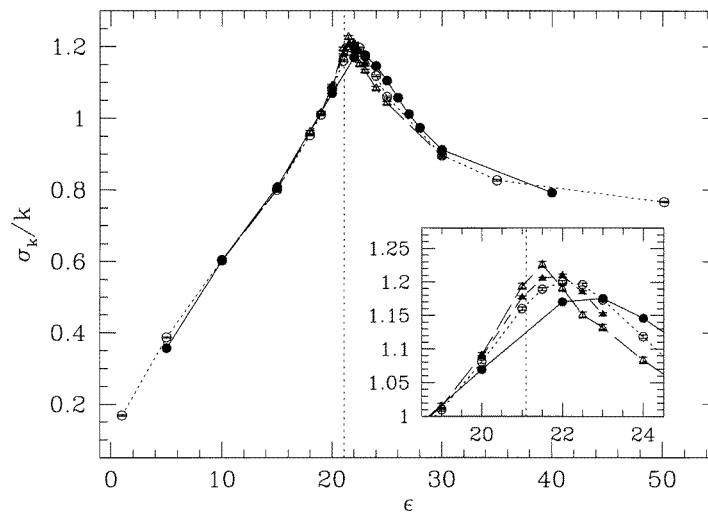


**Figure 16.** Normalized Ricci curvature fluctuations  $\sigma_k/k$  with Eisenhart metric versus energy density  $\epsilon$  for different sizes of the system. The symbols are the same as in figure 15.

## 6.2. Other geometric observables

The same analysis of the time-averaged geometric quantities can be carried on also in the framework of the Jacobi metric—equation (22). In this case the ambient space is the accessible configuration space. We have studied the behaviour of the time average and of the fluctuations of the scalar curvature, whose corresponding dynamical observable is

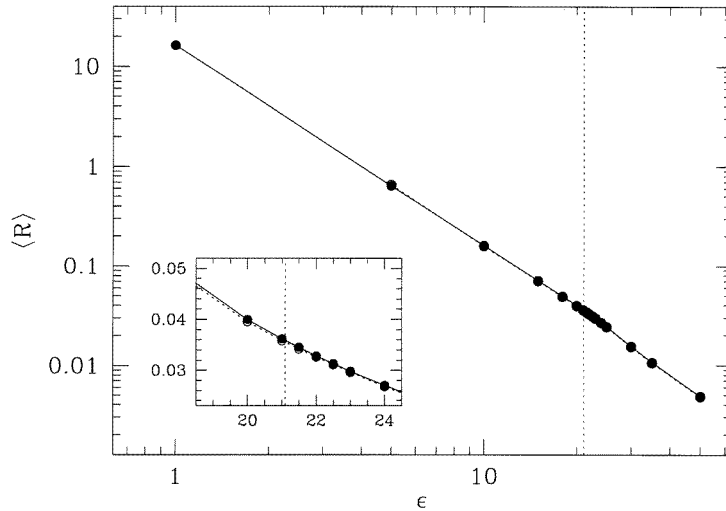


**Figure 17.** Average scalar curvature  $\langle R \rangle$  (34) with Jacobi metric versus energy density  $\varepsilon$  for different sizes of the system. The symbols denote respectively  $N = 10^2$  (full circles) and  $N = 20^2$  (open circles). The vertical dotted line marks the estimated value of  $\varepsilon_c$ . The inset shows a magnification of the transition region.

[3, 19]

$$\mathcal{R} = \frac{N-1}{4(E-V)^2} [2(E-V)\Delta V - (N-6)|\nabla V|^2]. \quad (34)$$

The results are reported in figures 17 and 18. We see that also with the Jacobi metric the average curvature seems to have a smooth behaviour near  $\varepsilon_c$ , even if in the two phases the overall behaviours of the curvature seem different; in contrast, the normalized fluctuation shows a sharp increase near criticality. Notice that these results have been obtained for small lattices only (up to  $20 \times 20$ ) hence, in analogy with the other observables, we expect that in larger lattices this effect should be even more pronounced.

Heretofore geometry has been introduced through dynamics, by identifying the dynamical trajectories with the geodesics of suitable manifolds.

However, other complementary approaches are also possible and interesting. Let us consider in particular the following one, recently introduced [39] in connection with the existence of different regimes in the dynamics of natural Hamiltonian systems. Given the dynamics, one can study the geometry of the trajectories as curves in the phase space, endowed with the Euclidean metric. In this way the trajectories are no longer geodesics of any manifold. Nevertheless, being the Hamiltonian trajectories constrained on the constant-energy hypersurface  $\Sigma_E$ , the geometry of such curves carries information on the ‘shape’ of the invariant hypersurface. Such a relation can be made precise in terms of the geometry of  $\Sigma_E$  seen as a submanifold of  $\mathbb{R}^n$  [19]. Let us define the curvature of the trajectory  $x(t) = (\varphi_1(t), \dots, \varphi_N(t), \pi_1(t), \dots, \pi_N(t))$  in phase space as the generalization to  $n = 2N$  dimensions of the curvature of a curve in the two-dimensional Euclidean plane:

$$\kappa = \frac{d\tau}{ds} \quad (35)$$

where  $\tau$  is the unit tangent vector to the curve  $x(t)$ , i.e.  $\tau = \dot{x}/|\dot{x}|$ , and  $s$  is the arc-length induced on  $x$  by the Euclidean metric of  $\mathbb{R}^n$ , hence  $ds/dt = |\text{grad } \mathcal{H}|$ .

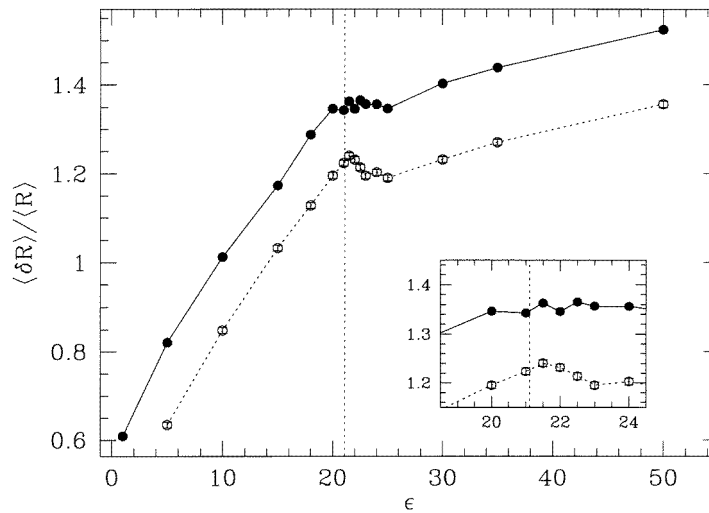


**Figure 18.** Normalized scalar curvature fluctuations  $\langle \delta \mathcal{R} \rangle / \langle \mathcal{R} \rangle$  with Jacobi metric versus energy density  $\varepsilon$  for different sizes of the system. The symbols are the same as in figure 17.

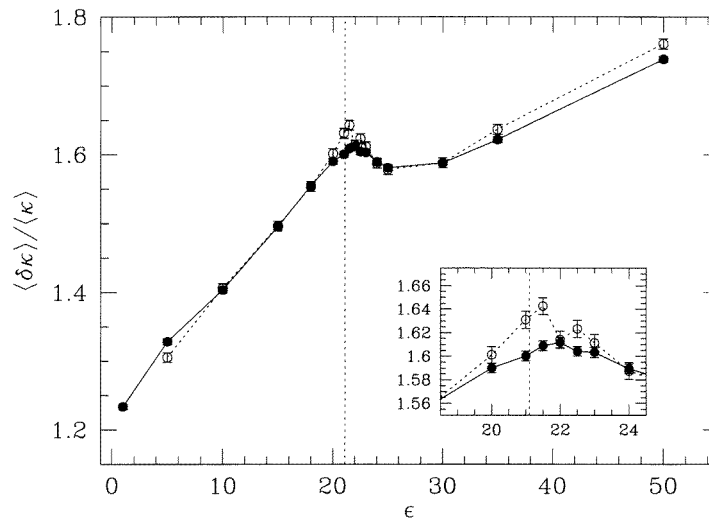


**Figure 19.** Normalized curvature fluctuations  $\langle \delta \kappa \rangle / \langle \kappa \rangle$  of the trajectories in phase space versus energy density  $\varepsilon$  for two different sizes of the system:  $N = 10^2$  (full circles) and  $N = 20^2$  (open circles).

The time average and the fluctuations of the observable  $\kappa$  can be defined as usual. In particular, the result for the normalized fluctuation  $\langle \delta^2 \kappa \rangle / \langle \kappa \rangle$  is reported in figure 19 for the two-dimensional  $\varphi^4$  model on a square lattice. We observe that the fluctuation of this curvature has a cusp-like behaviour in correspondence of the transition. Again we stress that this ‘quasisingular’ behaviour is already obtained with extremely small lattices.

The phenomenology summarized above suggests that in correspondence with a phase transition, the geometry of the manifolds underlying the dynamics undergoes a dramatic change. The precise nature of this change is still to be understood. Nevertheless, the

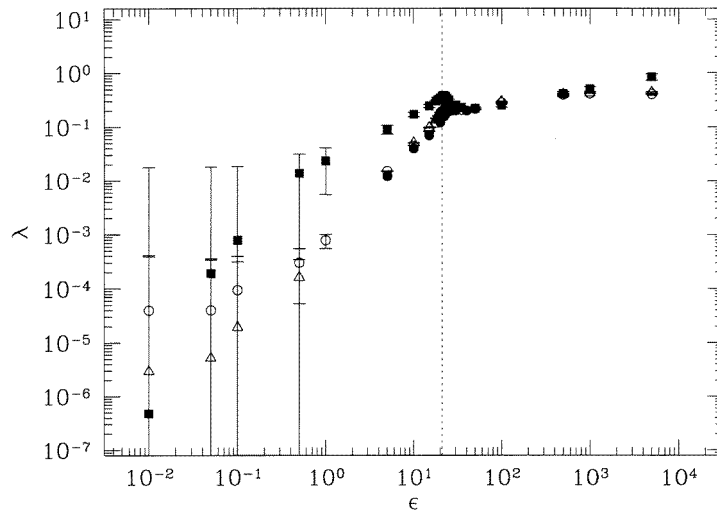


**Figure 20.** Synopsis of the geometric prediction of the Lyapunov exponent according to equation (31) (full squares) and of the numerical simulation results already plotted in figure 14.

fact that the singular behaviour of the curvature fluctuations shows up using *different* geometric settings indicates that it is a consequence of some *deeper* property: the topological interpretation of these phenomena [9] is strongly supported.

### 6.3. Geometric observables and Lyapunov exponents

The geometric observables considered in section 6.1 can be used to estimate the Lyapunov exponents. The result obtained applying equation (31) to the two-dimensional  $\varphi^4$  model are reported in figure 20. The agreement between theory and simulations is qualitatively good, but not from a quantitative point of view. A very good agreement is found only in an energy range of about two decades just above the transition. We do not have, at present, a deep explanation. A tentative one might involve the fact that in these models, especially close to the transition, the manifolds might be highly anisotropic (as witnessed by the growth of the curvature fluctuations) and thus the quasi-isotropy assumption may no longer be valid. Moreover, finite-size effects are expected to play a significant role. However, the nonsatisfactory agreement between theory and simulation for the Lyapunov exponent is not a common feature of all models with phase transitions. In fact, in the case of the two- and three-dimensional  $XY$  models the geometric estimate of the Lyapunov exponent is in very good agreement with the simulations [9]. Moreover, the analytical results obtained in [35] compare well with simulations. In [20] it has also been shown that in the case of  $\varphi^4$  models the estimate could be improved by adjusting the values of the timescale  $\tau$  in equation (31).

## 7. Concluding remarks

The first result of this work is that the statistical behaviour emerging from the microscopic Hamiltonian dynamics of a two-dimensional  $\varphi^4$  model is perfectly consistent with the predictions of equilibrium statistical mechanics, and the agreement between the two descriptions includes critical behaviour. This means that all the tools coming from Hamiltonian mechanics can be used to investigate phase transitions. One of the aspects that



can be considered in this perspective is certainly the possibility of an *ab initio* description of critical slowing down.

A further result is that the study of intrinsically dynamical observables, as Lyapunov exponents, reveals an intriguing relationship between the local instability properties of the phase-space dynamics and the global phenomenon of the phase transition. In this perspective it is worth mentioning a recently proposed approach [40] that unifies the description of Hamiltonian dynamics with the description of its stability through a path-integral formalism: this could be a way to relate stability properties with the phase transition from a general point of view. Here we approached this problem via a geometrization of the dynamics based on simple Riemannian tools. We found that the fluctuations of the curvatures of suitably defined manifolds associated with the Hamiltonian dynamics exhibit a ‘singular’ behaviour at the transition. This fact is coherent with the results recently found for other models undergoing a phase transition, as the lattice  $\varphi^4$  theory in three space dimensions, with both  $\mathbb{Z}_2$  and  $O(n)$  symmetries [20], and the classical  $XY$  Heisenberg model in two and three space dimensions [9, 41].

A topological conjecture has been proposed to explain this behaviour [9]: the phase transition could be a consequence of a major topological change in the manifolds where the dynamical trajectories live. Such a conjecture receives further support from the results presented here, also because an apparently singular behaviour in the curvature fluctuations is also found using different geometric settings with respect to those used in the previous works, which were all based on the Eisenhart metric. The problem of a precise characterization of these topological changes is still open and work is in progress in this direction (see [19] for some preliminary results).

## Acknowledgments

We thank S Caracciolo, C Clementi, E G D Cohen, M-C Firpo, R Gatto, R Livi, M Modugno, G Pettini, M Rasetti and S Ruffo for fruitful discussions and for their interest and support. Large parts of this work have been done while LC was a PhD student at the Scuola Normale Superiore, Pisa, Italy, and visiting fellow at the Département de Physique Théorique, Université de Genève, Switzerland. The ISI Foundation in Torino, Italy, is also acknowledged for its kind hospitality.

## References

- [1] Fermi E, Pasta J and Ulam S 1965 *Collected Papers of Enrico Fermi* vol 2, ed E Segré (Chicago, IL: University of Chicago) p 978
- [2] Gutzwiller M C 1977 *J. Math. Phys.* **18** 806  
van Velsen J F C 1980 *J. Phys. A: Math. Gen.* **13** 833  
Savvidy G K 1984 *Nucl. Phys. B* **246** 302  
Knauf A 1987 *Commun. Math. Phys.* **110** 89
- [3] Pettini M 1993 *Phys. Rev. E* **47** 828
- [4] Casetti L and Pettini M 1993 *Phys. Rev. E* **48** 2340
- [5] Cerruti-Sola M and Pettini M 1995 *Phys. Rev. E* **51** 53  
Cerruti-Sola M and Pettini M 1996 *Phys. Rev. E* **53** 179
- [6] Pettini M and Valdetaro R 1995 *Chaos* **5** 646
- [7] Casetti L, Livi R and Pettini M 1995 *Phys. Rev. Lett.* **74** 375
- [8] Casetti L, Clementi C and Pettini M 1996 *Phys. Rev. E* **54** 5969
- [9] Caiani L, Casetti L, Clementi C and Pettini M 1997 *Phys. Rev. Lett.* **79** 4361
- [10] Antoni M and Ruffo S 1995 *Phys. Rev. E* **52** 2361
- [11] Elskens Y and Antoni M 1997 *Phys. Rev. E* **55** 6575

- [12] Rugh H H 1997 *Phys. Rev. Lett.* **78** 772
- [13] Giardinà C and Livi R 1997 *Preprint* chao-dyn/9709015 submitted to *J. Stat. Phys.*
- [14] Gross D H E and Madjet M E 1996 *Preprint* cond-mat/9611192
- [15] Dellago Ch, Posch H A and Hoover W G 1996 *Phys. Rev. E* **53** 1485  
Dellago Ch and Posch H A 1996 *Physica* **230A** 364
- [16] Hohenberg P C and Halperin B I 1977 *Rev. Mod. Phys.* **49** 435
- [17] Goldenfeld N 1992 *Lectures on Phase Transitions and the Renormalisation Group* (New York: Addison-Wesley)
- [18] Butera P and Caravati G 1987 *Phys. Rev. A* **36** 962
- [19] Casetti L 1997 Aspects of dynamics, geometry and statistical mechanics in Hamiltonian systems *PhD Thesis* (Pisa: Scuola Normale Superiore) available at the URL  
<http://www.sns.it/html/ClasseScienze/ThPhysics.html>
- [20] Caiani L, Casetti L, Clementi C, Pettini G, Pettini M and Gatto R 1998 *Phys. Rev. E* **57** to appear
- [21] Casetti L 1995 *Phys. Scr.* **51** 29
- [22] Khinchin A Ya 1949 *Mathematical Foundations of Statistical Mechanics* (New York: Dover)
- [23] Pearson E M, Halicioglu T and Tiller W A 1985 *Phys. Rev. A* **32** 3030
- [24] Lebowitz J, Percus J and Verlet L 1967 *Phys. Rev.* **153** 250
- [25] Binder K and Ciccotti G (ed) 1996 Monte Carlo and molecular dynamics of condensed matter systems *Proc. Euroconf. and Summer School (Villa Olmo, Como, July 1995)* (Bologna: Editrice Compositori)
- [26] Frenkel D 1996 *Proc. Euroconf. and Summer School (Villa Olmo, Como, July 1995)* ed K Binder and G Ciccotti (Bologna: Editrice Compositori)
- [27] Dunweg B 1996 *Proc. Euroconf. and Summer School (Villa Olmo, Como, July 1995)* ed K Binder and G Ciccotti (Bologna: Editrice Compositori)
- [28] Binder K 1981 *Z. Phys. B* **43** 119
- [29] Young A P 1996 *Proc. Euroconf. and Summer School (Villa Olmo, Como, July 1995)* ed K Binder and G Ciccotti (Bologna: Editrice Compositori)
- [30] Sokal A 1989 Monte Carlo methods: foundations and new algorithms *Cours de 3<sup>ème</sup> Cycle de la Physique en Suisse Romande (Lausanne)*
- [31] Bonasera A, Latora V and Rapisarda A 1995 *Phys. Rev. Lett.* **75** 3434
- [32] O'Hern C S, Egolf D A and Greenside H S 1996 *Phys. Rev. E* **53** 3374
- [33] Mehra V and Ramaswamy R 1997 *Preprint* chao-dyn/9706011
- [34] Latora V, Rapisarda A and Ruffo S 1998 *Phys. Rev. Lett.* **80** 692
- [35] Firpo M-C 1998 *Phys. Rev. E* **57** to appear
- [36] Krylov N S 1979 *Works on the Foundations of Statistical Mechanics* (Princeton, NJ: Princeton University Press)
- [37] Eisenhart L P 1929 *Ann. Math.* **30** 591
- [38] do Carmo M P 1993 *Riemannian Geometry* (Boston, MA: Birkhäuser)
- [39] Alabiso C, Besagni N and Casartelli M 1996 *J. Phys. A: Math. Gen.* **29** 3733
- [40] Gozzi E and Reuter M 1989 *Phys. Lett. B* **233** 383  
Gozzi E, Reuter M and Thacker W D 1992 *Chaos, Solitons Fractals* **2** 441  
Gozzi E and Reuter M 1994 *Chaos, Solitons Fractals* **4** 1117
- [41] Clementi C 1995 *Laurea Thesis* University of Florence, Italy